

## ParaCEST MRI contrast agents capable of derivatization *via* “click” chemistry†

Mark Milne,<sup>a</sup> Kirby Chicas,<sup>a</sup> Alex Li,<sup>b</sup> Robert Bartha<sup>b</sup> and Robert H. E. Hudson<sup>\*a</sup>

Received 13th July 2011, Accepted 26th September 2011

DOI: 10.1039/c1ob06162c

A comprehensive series of lanthanide chelates has been prepared with a tetrapropargyl DOTAM type ligand. The complexes have been characterized by a combination of <sup>1</sup>H NMR, single-crystal X-ray crystallography, CEST and relaxation studies and have also been evaluated for potential use as paramagnetic chemical exchange saturation transfer (ParaCEST) contrast agents in magnetic resonance imaging (MRI). We demonstrate the functionalization of several chelates by means of alkyne–azide “click” chemistry in which a glucosyl azide is used to produce a tetra-substituted carbohydrate-decorated lanthanide complex. The carbohydrate periphery of the chelates has a potent influence on the CEST properties as described herein.

### Introduction

Cyclen-based chelates of lanthanide ions, particularly gadolinium although other metals are being actively investigated, are widely used as contrast agents in magnetic resonance imaging (MRI). These agents rely on the exchange of water between the bulk and the coordination sphere of the lanthanide.<sup>1–7</sup> The exchange rate of bound water depends both on the nature of the ligand and the identity of the metal ion. The exchange rate of bound water has been described as fast in 1,4,7,10-tetrakis(carboxymethyl)-1,4,7,10-tetraazacyclododecane (DOTA) type ligands, or slow-to-intermediate, as in 1,4,7,10-tetraazacyclododecane-1,4,7,10-tetraacetamide (DOTAM) type ligands. Due to these two possible exchange rate regimes, two different techniques have been developed to create contrast in MRI. Fast exchange occurs when Gd<sup>3+</sup> is used in combination with DOTA type ligands wherein the change in *T*<sub>1</sub> is used to produce the contrast. Alternatively, contrast agents in the slow-to-intermediate exchange regime, such as the combination of DOTAM type ligands and Eu<sup>3+</sup>, use the paramagnetic chemical exchange saturation transfer (ParaCEST) phenomenon to produce contrast. Not only does the exchange rate depend on the gross chemical features of the ligand, it is also sensitive to the geometry of the chelator about the metal centre. It has been described that cyclen-based contrast agents are found in either a twisted square antiprismatic (TSAP) form, in which exchange is fast, or in a square antiprismatic (SAP) form in which the exchange is slower.<sup>1,6–10</sup> In order to maximize the ParaCEST

signal, it is desirable to have ligands which exist only in the SAP geometry.

Development of targeted contrast agents using glycoconjugates have been studied recently. A number of different synthetic approaches have been investigated producing contrast agents ranging from those possessing a single saccharide up to dendrimeric structures containing twelve glucose moieties.<sup>11–14</sup> Most of these agents have relied on Gd<sup>3+</sup> to produce contrast using the theory of relaxivity as previously discussed. The use of other lanthanides which produce large chemical shifts suitable for use in ParaCEST experiments have not been exploited to the same extent. By incorporating metal ions that are compatible with the ParaCEST approach, we are able to measure the metal-bound water of Eu<sup>3+</sup> complexes, as well as the exchangeable amide protons in the other lanthanide complexes (especially Dy<sup>3+</sup>, Tm<sup>3+</sup> and Tb<sup>3+</sup>). The latter group of lanthanides have elicited interest lately due to the sensitivity of amide proton exchange to changes in pH and the potential for *in vivo*, non-invasive pH measurement. The potential for the measurement of physiological parameters, such as pH, is one of the advantages of ParaCEST agents over conventional *T*<sub>1</sub> agents. Determination of *in vivo* pH has implications for the early detection of cancerous tissue which is known to be acidic compared to healthy tissue.<sup>15,16</sup> A second benefit of using the signal from exchangeable amide protons is the increased CEST sensitivity compared to bound water due to the greater number of equivalent protons, provided that the contrast agent is symmetrical.<sup>17</sup>

### Results and discussion

A recent publication<sup>18</sup>‡ on related compounds has prompted us to report our ongoing studies on the structure and properties of

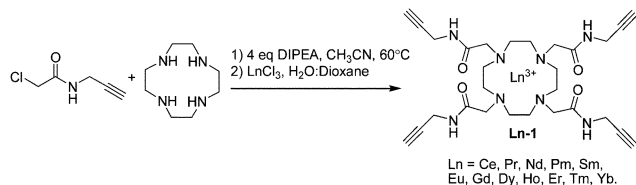
<sup>a</sup>Department of Chemistry, The University of Western Ontario, London, Ontario, CANADA, N6A 5B7. E-mail: robert.hudson@uwo.ca; Fax: +1-519-661-3022; Tel: +1-519-661-2111 ext. 86349

<sup>b</sup>Department of Medical Biophysics, The University of Western Ontario, London, Ontario, CANADA, N6A 5K8

† Electronic supplementary information (ESI) available. CCDC reference numbers 814847–814850. For ESI and crystallographic data in CIF or other electronic format see DOI: 10.1039/c1ob06162c

‡ A value 2.83 mM<sup>-1</sup> s<sup>-1</sup> for *r*<sub>1</sub> at 400 MHz of Gd-1 has been recently reported (ref. 18).

a tetrapropargyl DOTAM series of lanthanide complexes toward the development of new contrast agents.<sup>19</sup> The synthesis of the DOTAM ligands was accomplished by modification of a literature procedure (Scheme 1).<sup>20</sup>



**Scheme 1** Synthesis of Ln-1.

Complexation of the lanthanide metal series was carried out by adding 1.1 equiv. of appropriate LnCl<sub>3</sub> (Ln<sup>3+</sup> = Ce, Pr, Nd, Sm, Eu, Gd, Tb, Dy, Ho, Er, Tm, Yb) to the tetrapropargyl DOTAM ligand in 2 mL of a 1 : 1 mixture of dioxane : H<sub>2</sub>O followed by overnight stirring. The solvent was evaporated and the solids were taken up in 1 mL H<sub>2</sub>O and passed through a column of size exclusion gel to remove free Ln<sup>3+</sup> ions which was confirmed by the xylenol orange test. The solvent was evaporated to yield Ln<sup>3+</sup> complexes. Conformational analysis was done by solution <sup>1</sup>H NMR, Fig. 1 and Table 1. The signal at ~25 ppm (**Eu-1**) is characteristic of SAP geometry and the lack of a signal at 8–10 ppm indicates the absence of the TSAP isomer in solution.<sup>8,21</sup>

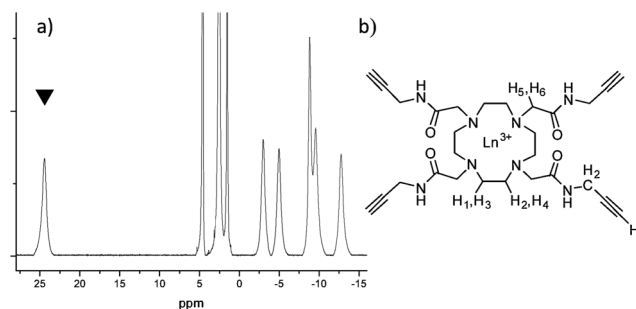


**Fig. 1** (a) <sup>1</sup>H NMR spectra of **Eu-1** (D<sub>2</sub>O, 600 MHz). H<sub>4</sub> indicated by arrowhead. (b) Designation of ligand hydrogen atoms (H<sub>1</sub>–H<sub>6</sub>) present in the Ln-1 complexes.

The solution phase NMR data taken together with solid state X-ray crystal structures (**Nd-1**, **Tb-1**, **Dy-1**, **Yb-1**, Fig. 2), indicate that only the SAP isomer is present for the lanthanide series of tetraalkyne DOTAM.

**Table 1** <sup>1</sup>H NMR chemical shifts (ppm) at 25 °C for the Ln<sup>3+</sup> series

Ln	H <sub>1</sub>	H <sub>2</sub>	H <sub>3</sub>	H <sub>4</sub>	H <sub>5</sub>	H <sub>6</sub>	CH <sub>2</sub>	CH
Ce <sup>3+</sup>	6.71	1.66	0.75	−7.58	7.45	5.17	4.97	4.97
Pr <sup>3+</sup>	14.09	3.22	0.79	−22.65	16.99	10.76	6.69	3.82
Nd <sup>3+</sup>	10.61	5.62	5.02	−11.38	12.34	5.62	7.46	5.48
Sm <sup>3+</sup>	4.39	1.61	1.79	−0.02	5.93	3.72	4.30	2.79
Eu <sup>3+</sup>	−9.58	−2.98	−4.98	24.43	−12.76	−8.83	2.57	1.53
Tb <sup>3+</sup>	104.74	−80.15	−83.30	−310.02	202.11	57.05	35.58/30.82	19.61
Dy <sup>3+</sup>	123.52	−83.04	−83.04	−356.08	234.87	77.18	38.76/33.88	22.04
Ho <sup>3+</sup>	65.27	−47.36	−43.19	−181.61	122.53	35.31	22.17/19.55	12.55
Er <sup>3+</sup>	−34.82	2.20	11.69	106.08	−61.37	−39.64	−2.50	−2.82
Tm <sup>3+</sup>	−85.88	30.33	40.30	247.40	−156.17	−74.56	−12.18/−13.22	−9.87
Yb <sup>3+</sup>	−30.64	14.19	17.14	94.09	−55.40	−25.15	−2.23	−2.58

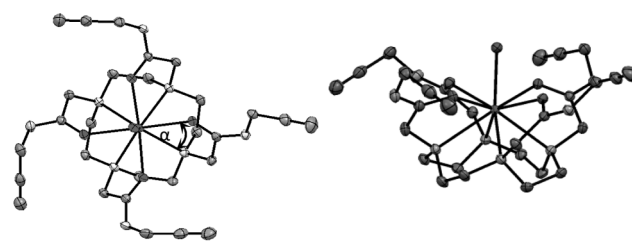


**Fig. 2** (Left) Top down view of ORTEP representation of **Dy-1**.  $\alpha$  indicates the angle between the planes created by N–Ln–N and O–Ln–O and are listed in Table 2. (Right) Side on view showing water coordinated to the metal centre, the positions of hydrogen atoms were not determined experimentally and are omitted for clarity.

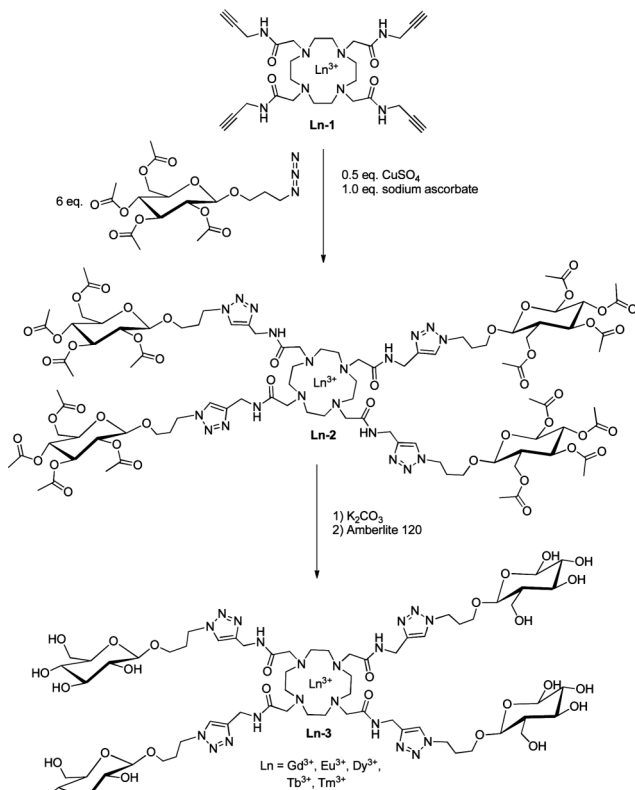
The lanthanide tetraalkyne DOTAM complexes possess non-planar conformations with C<sub>4</sub> symmetry which can be identified by the presence of 8 proton signals, denoted H<sub>1</sub> to H<sub>6</sub>, CH<sub>2</sub> (propargylic methylene) and CH (terminal proton). Those protons closer to the metal centre exhibit higher chemical shifts than in the free ligand due to the magnetic moment of the metal centres (Table 1).<sup>21</sup> Of note, the protons for the CH<sub>2</sub> group for Dy<sup>3+</sup>, Ho<sup>3+</sup>, Tb<sup>3+</sup> and Tm<sup>3+</sup> compounds show two separate peaks, where the rest of the metals show a single peak. This is likely due to the large shift capabilities of these four compounds resolving the diastereotopic protons. Proton analysis was not performed for the **Gd-1** complex due to line broadening.

These results are notable, particularly, when compared to other high chemical shift lanthanide complexes which have shown two isomers in solution.<sup>8</sup> The SAP isomer is desirable for two reasons: firstly, it produces greater hyperfine shifts of the ligand (cyclen) associated protons that may be useful for magnetic resonance spectroscopic applications. Secondly, the SAP isomer has the slower water exchange rate of the two isomers and this feature is important for ParaCEST-based contrast agents.

To illustrate the competence of the DOTAM alkyne to be derivatized, we have taken tetraacetylglucosyl propylazide and performed a copper-catalyzed azide–alkyne 1,3 dipolar cycloaddition (CuACC) or “click”<sup>22</sup> reaction to give a tetra glucose (OAc)<sub>4</sub>.<sup>23</sup> This chemistry was performed on a series of pre-metallated ligand (**Ln-1**, Ln = Eu<sup>3+</sup>, Dy<sup>3+</sup>, Tm<sup>3+</sup>, Tb<sup>3+</sup>, Gd<sup>3+</sup>) to avoid metal sequestration by the naked ligand and subsequent need for transmetalation.

The acetyl-protected glucose intermediates **Ln-2** were purified by HPLC, with similar retention times being observed for all metals, and isolated in 60–82% yield, while their identities were

confirmed by high resolution mass spectrometry. The glucose moieties were deacetylated using a catalytic amount of potassium carbonate in methanol and this reaction was subsequently quenched by stirring with Amberlite 120 resin. This treatment afforded the fully deprotected tetraglucoside (**Ln-3**) products in high yield (99%) (Scheme 2).



**Scheme 2** Synthesis of a tetraglucoside functionalized DOTAM *via* the acetyl-protected intermediate by Huisgen copper-catalyzed alkyne–azide cycloaddition (CuAAC).

A selection of lanthanides was used in the click reactions based on their potential as contrast agents.  $Gd^{3+}$  was chosen for its ability as a  $T_1$  relaxation agent while the other lanthanides ( $Eu^{3+}$ ,  $Dy^{3+}$ ,  $Tb^{3+}$ ,  $Tm^{3+}$ ) were chosen because of their favourable characteristics as ParaCEST contrast agents.

To evaluate the series of complexes as potential contrast agents for MRI, relaxation measurements and CEST experiments were made. NMRD profiles were acquired at 25 °C using a STELLAR fast field cycling NMR (Fig. S13–S15†). CEST spectra were acquired at 25 °C, at 10 mM in phosphate buffer (pH 7) and show observable signals due to bound water and amide protons (Fig. S16–S24†).

The measured  $r_1$  value at 20 MHz for **Gd-1** ( $2.53 \text{ mM}^{-1} \text{ s}^{-1}$ ) is comparable to the value previously reported for  $Gd^{3+}$ -DOTAM ( $2.5 \text{ mM}^{-1} \text{ s}^{-1}$ ).<sup>6</sup> The relaxivity of the products of the “click” reaction, the tetrakis(tetra-*O*-acetylglycoside) **Gd-2** and the deacetylated congener **Gd-3**, were also evaluated (Table 2). An  $r_1$  value of  $1.96 \text{ mM}^{-1} \text{ s}^{-1}$  at 20 MHz, 25 °C was obtained for **Gd-2** while a slightly higher value of  $2.08 \text{ mM}^{-1} \text{ s}^{-1}$  was obtained for compound **Gd-3** (Fig. S27†). The relaxivities measured at 400 MHz displayed a similar trend in that **Gd-1** possessed the

**Table 2** Relaxivities of  $Gd^{3+}$  complexes ( $\text{mM}^{-1} \text{ s}^{-1}$ )

$Ln^{3+}$	$r_1$ (20 MHz)	$r_1$ (400 MHz)
<b>Gd-1</b>	2.53	2.22
<b>Gd-2</b>	1.96	1.96
<b>Gd-3</b>	2.08	2.13

greatest value ( $2.22 \text{ mM}^{-1} \text{ s}^{-1}$ ) while a decrease was observed for **Gd-2** ( $1.96 \text{ mM}^{-1} \text{ s}^{-1}$ ) and an increase for **Gd-3** ( $2.13 \text{ mM}^{-1} \text{ s}^{-1}$ ), as compared to **Gd-2** (Fig. S28†).

Despite the magnitude of the changes in relaxivity being modest, the pattern of change is somewhat surprising. Relaxivity theory states that as the size of the contrast agent increases, at low field strengths, so should the rotational time, ultimately giving rise to an increase in relaxivity.<sup>24</sup> This, however, is not the pattern observed for the  $Gd^{3+}$  series at 20 MHz. On the basis of molecular mass, **Gd-2** is approximately 3 times larger than **Gd-1** but a decrease in relaxivity of 22% was measured. This unusual situation is also observed when comparing **Gd-2** and **Gd-3** where relaxivity was observed to increase by 6% while the molecular mass decreased by 27%. While these changes in relaxivity are modest and may be due to experimental error it should be noted that similar results have been shown for other glycoconjugates, where tripling the size gave rise to only marginal increases in relaxivity.<sup>14</sup> These results may be understood by assuming that the rotational time is not the predominant factor associated with the relaxivity. Instead the water exchange rate or accessibility of metal-coordinated water to the bulk is a more important determining factor for relaxivity in the slow-to-intermediate exchange regime of DOTAM ligands.

The dependence on water access to the metal centre and the core of the ligand is also reflected in the results from the CEST experiments for both the bound water ( $Eu^{3+}$  series) and exchangeable amide protons ( $Tm^{3+}$  series). CEST experiments were performed on complexes **Eu-(1–3)**, **Tb-(1–3)**, **Tm-(1–3)**, and **Dy-(1–3)** to evaluate their potential to act as ParaCEST contrast agents, Tables 3 and 4. The  $Eu^{3+}$ ,  $Tb^{3+}$ ,  $Tm^{3+}$  and  $Dy^{3+}$  complexes of ligand **1** all show CEST signals. Signals due to exchangeable amide protons are observed for **Tb-1** and **Dy-1** (both 14%) and for **Tm-1** (16%) while exchangeable, metal coordinated water is observed for **Dy-1** (4.4%), **Tb-1** (5.4%) and **Eu-1** (40%). These results are comparable to previously reported Ln DOTAM ligands. **Dy-DOTAM** amide (80 ppm, 15%) and **Eu-DOTAM** water (50 ppm, 30%).<sup>17</sup>

Subsequent to the CuACC, the hydrophobic nature of the complexes was increased due to the attachment of per-acetylated glucose moieties. The observed CEST response for **Eu-2** ( $H_2O$ , 18%) and **Tm-2** (amide, 2%) were both diminished in comparison

**Table 3** Chemical shifts and CEST signals of exchangeable amides

$Ln^{3+}$	$\delta$ (ppm) amide	CEST (%) amide
<b>Dy-DOTAM<sup>a</sup></b>	80	15
<b>Dy-1</b>	81	14
<b>Tb-1</b>	65	14
<b>Tm-1</b>	-54	16
<b>Tm-2</b>	-49	2
<b>Tm-3</b>	-51	6

<sup>a</sup> pH 6.92, 10 mM,  $B_0 = 500 \text{ MHz}$ , 25 °C,  $B_1 = 1000 \text{ Hz}$ , Pre-sat time = 2 s.<sup>17</sup>

**Table 4** Chemical shifts and CEST signals of bound water

Ln <sup>3+</sup>	$\delta$ (ppm) H <sub>2</sub> O	CEST (%) H <sub>2</sub> O
<b>Eu-DOTAM<sup>a</sup></b>	50	30
<b>Dy-1</b>	-765	4.4
<b>Tb-1</b>	-640	5.4
<b>Eu-1</b>	51	40
<b>Eu-2</b>	52	18
<b>Eu-3</b>	53	23

<sup>a</sup> pH 7.0, 10 mM, B<sub>0</sub> = 500 MHz, 25 °C, B<sub>1</sub> = 1000 Hz, Pre-sat time = 2 s.<sup>17</sup>

to the parent alkyne complexes. After deprotection of the glucose units, there was an increase of 5% and 4% observed for **Eu-3** (Fig. 3) and **Tm-3** respectively (Fig. S29, S30<sup>†</sup>). CEST signals for **Dy-(2,3)** and **Tm-(2,3)** were not observed for either the amide proton or bound water.

These results are congruent with the explanation propounded for the trends in relaxivity. The CEST effect should be relatively insensitive to rotational effects, thus the observed changes in CEST signals are accounted for by changes in accessibility of bulk water to exchange with the metal-bound water or the amide protons of the ligand framework. The acetylated glucose-decorated ligand possesses a greater barrier between the metal-coordinated and bulk water compared to the deacetylated ligand, which in turn is greater than the parent **Ln-1** complexes. Because DOTAM-based contrast agents are in a slow-to-intermediate exchange regime the CEST response and the relaxivity are both sensitive to the hydrophobicity of the agents and less responsive to the size change and rotational time.

Crystals suitable for X-ray diffraction were grown by slow diffusion of acetone into a concentrated aqueous solution of the complexes. All of the crystal structures displayed nine-fold coordination of the metal centre consisting of four nitrogens from cyclen, four oxygens from the pendant arms, and the last coordination site occupied by a single water molecule of varying bond length (Nd = 2.47 Å, Tb = 2.44 Å, Dy = 2.43 Å, Yb = 2.42 Å). The angle between the planes of N–Ln–N and O–Ln–O was found to be between 37 and 39° for all crystals, indicating a SAP geometry in the solid state. Selected bond lengths and angles are summarised in Table 5 and are comparable to previously reported similar DOTAM crystals.<sup>18</sup> N–Ln distances of ~2.65 Å and O–Ln distances of 2.35 Å are comparable to previously reported Gd DOTA crystals.<sup>25</sup> Crystallography data are summarized in Table 6.

**Table 5** Summary of torsion angle of pendent arms  $\alpha$  (°) and key bond lengths (Å)

	Nd-1	Tb-1	Dy-1	Yb-1
$\alpha$ angle	37.48	38.94	39.04	39.51
N <sub>2</sub> –C–O <sub>1</sub>	22.8	35.1	30.0	22.9
N <sub>3</sub> –C–O <sub>2</sub>	35.8	30.1	28.3	34.0
N <sub>5</sub> –C–O <sub>3</sub>	28.3	28.4	23.3	30.1
N <sub>7</sub> –C–O <sub>4</sub>	30.7	23.2	34.6	28.3
N <sub>2</sub> –Ln	2.70	2.65	2.64	2.60
N <sub>3</sub> –Ln	2.70	2.65	2.60	2.62
N <sub>5</sub> –Ln	2.72	2.61	2.63	2.61
N <sub>7</sub> –Ln	2.66	2.64	2.64	2.57
O <sub>1</sub> –Ln	2.43	2.36	2.35	2.30
O <sub>2</sub> –Ln	2.48	2.36	2.41	2.30
O <sub>3</sub> –Ln	2.41	2.36	2.35	2.36
O <sub>4</sub> –Ln	2.45	2.42	2.35	2.36
H <sub>2</sub> O–Ln	2.47	2.44	2.43	2.42

## Experimental

CEST spectra were acquired on a 9.4 T scanner with the following parameters, FOV (field of view): 25.6 × 25.6 mm<sup>2</sup>, matrix 128 × 128, flash pulse, TR: 6 ms, TE: 3 ms, flip angle: 6°. The bound water ParaCEST spectra for Eu<sup>3+</sup>, Tb<sup>3+</sup> and Dy<sup>3+</sup> were acquired by applying a presaturation pulse at 15  $\mu$ T for 4 s in steps of 5 ppm from -1000 to 1000 ppm. Amide exchange spectra (Tb<sup>3+</sup>, Tm<sup>3+</sup> and Dy<sup>3+</sup>) were acquired by applying a presaturation pulse at 15  $\mu$ T for 4 s in steps of 1 ppm from -100 to 100 ppm. All solvents were HPLC grade and used as such, except for dioxane and CH<sub>2</sub>Cl<sub>2</sub> (dried by passing through columns of activated Al<sub>2</sub>O<sub>3</sub>) and water (18.2 M $\Omega$  cm<sup>-1</sup> deionized). Organic extracts were dried with Na<sub>2</sub>SO<sub>4</sub> and solvents were removed under reduced pressure in a rotary evaporator. Size exclusion chromatography was carried out on BIO-GEL P2, 45–90 mesh resin (20 g, column size 15 × 2 cm per 0.1 mmol of compound). HPLC analysis was carried out using a high performance liquid chromatograph using a Microsorb-CN column (particle size 5  $\mu$ m; 4.6 id × 200 mm). Mobile phase: gradient: 80:20 H<sub>2</sub>O:CH<sub>3</sub>CN to 35:65 H<sub>2</sub>O:CH<sub>3</sub>CN over 8 min 35:65 H<sub>2</sub>O:CH<sub>3</sub>CN for 7 min. **Ln-2** (R<sub>t</sub> = 7.55 min). **Ln-3** (R<sub>t</sub> = 1.50 min) NMR spectra were recorded on a 400 MHz spectrometer; for <sup>1</sup>H (400 MHz), chemical shift values ( $\delta$ ) are reported relative to TMS and were referenced to the residual proton in the deuterated solvents as follows: CDCl<sub>3</sub> (7.26 ppm);

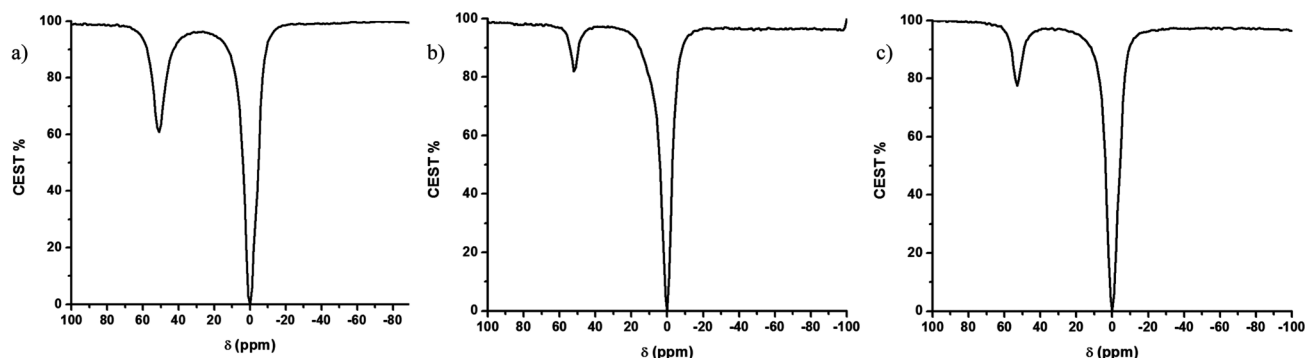


**Fig. 3** CEST spectra acquired at 10 mM, 25 °C, using a 15  $\mu$ T saturation pulse for 4 s: (a) **Eu-1**, (b) **Eu-2**, (c) **Eu-3**. Peak position and intensities are listed in Tables 3 and 4.

**Table 6** Crystallography data for Nd-1, Yb-1, Tb-1 and Dy-1

Compound reference	Tb-1	Dy-1	Nd-1	Yb-1
Chemical formula	C <sub>28</sub> H <sub>42</sub> N <sub>8</sub> O <sub>5</sub> Tb-(C <sub>3</sub> H <sub>15</sub> O <sub>5</sub> Cl <sub>3</sub> )	C <sub>28</sub> H <sub>42</sub> N <sub>8</sub> O <sub>5</sub> Dy-(C <sub>3</sub> H <sub>16</sub> O <sub>5</sub> Cl <sub>3</sub> )	C <sub>28</sub> H <sub>42</sub> N <sub>8</sub> O <sub>5</sub> Nd-(C <sub>3</sub> H <sub>16</sub> O <sub>5</sub> Cl <sub>3</sub> )	C <sub>28</sub> H <sub>42</sub> N <sub>8</sub> O <sub>5</sub> Yb-(C <sub>3</sub> H <sub>12</sub> O <sub>5</sub> Cl <sub>3</sub> )
Formula mass	967.12	971.70	953.44	977.20
Crystal system	Triclinic	Triclinic	Triclinic	Triclinic
<i>a</i> /Å	10.8916(5)	10.8844(4)	11.1524(6)	10.8858(5)
<i>b</i> /Å	14.3620(6)	14.3626(6)	13.9136(7)	14.3185(6)
<i>c</i> /Å	15.4604(10)	15.4658(10)	15.2106(12)	15.4483(7)
$\alpha$ (°)	113.338(2)	113.395(3)	110.878(3)	113.484(2)
$\beta$ (°)	103.205(3)	103.121(3)	103.133(3)	102.767(2)
$\gamma$ (°)	99.220(2)	99.252(2)	100.034(2)	99.404(2)
Unit cell volume/Å <sup>3</sup>	2075.04(19)	2074.15(18)	2061.4(2)	2067.00(16)
<i>T</i> /K	150(2)	150(2)	150(2)	150(2)
Space group	<i>P</i> $\bar{1}$	<i>P</i> $\bar{1}$	<i>P</i> $\bar{1}$	<i>P</i> $\bar{1}$
No. of formula units per unit cell, <i>Z</i>	2	2	2	2
No. of reflections measured	246 235	286 221	220 951	278 130
No. of independent reflections	10 723	12 145	9849	10 268
<i>R</i> <sub>int</sub>	0.0518	0.0682	0.0831	0.1154
Final <i>R</i> <sub>1</sub> values ( <i>I</i> > 2σ( <i>I</i> ))	0.0224	0.0237	0.0269	0.0303
Final <i>wR</i> ( <i>F</i> <sup>2</sup> ) values ( <i>I</i> > 2σ( <i>I</i> ))	0.0574	0.0593	0.0615	0.0631
Final <i>R</i> <sub>1</sub> values (all data)	0.0263	0.0289	0.0347	0.0431
Final <i>wR</i> ( <i>F</i> <sup>2</sup> ) values (all data)	0.0598	0.0620	0.0647	0.0683

DMSO-*d*<sub>6</sub> (2.49 ppm); D<sub>2</sub>O (4.75 ppm). Mass spectra (MS) were obtained using electrospray ionization (ESI).

#### *N*-(Propargyl) chloroacetamide

Chloroacetyl chloride (5.97 mL, 75 mmol) was added dropwise to a stirred solution of propargylamine HCl (455 mg, 50 mmol) and NaHCO<sub>3</sub> (12.75 g, 150 mmol) in 50 mL dry DCM. The solution was stirred for 3 h, filtered and washed with 5% NaHCO<sub>3</sub>. The organic layer was dried over MgSO<sub>4</sub> and dried under reduced pressure giving a brown solid (3.52 g, 27 mmol), yield 54%. <sup>1</sup>H NMR (400 MHz, CDCl<sub>3</sub>): δ 6.81 (1H, br, s); 4.10 (2H, m); 4.07 (2H, s); 2.28 (1H, t, *J* = 2.5 Hz).

#### Tetraalkyne DOTAM (1)

To a stirred solution of cyclen (267 mg, 1.5 mmol) and DIPEA (955 μL, 24.8 mmol) in 10 mL acetonitrile, *N*-(propargyl) chloroacetamide (816 mg, 6.2 mmol) was added in one portion and then refluxed overnight. The product was precipitated by the addition of 50 mL H<sub>2</sub>O and isolated by filtration. White solid (680 mg, 1.2 mmol), yield 76%. <sup>1</sup>H NMR (400 MHz, DMSO-*d*<sub>6</sub>): δ 7.57 (4H, m); 3.05 (8H, m); 2.22 (10H, m); 1.79 (14H, s); 1.67 (4H, s). ESI-TOF: *m/z* calcd for C<sub>28</sub>H<sub>40</sub>N<sub>8</sub>O<sub>4</sub> (M + H)<sup>+</sup>, 553.3251, found 553.2574.

#### Ln tetraalkyne DOTAM (Ln-1)

Tetraalkyne DOTAM (1) (55 mg, 0.1 mmol) was added to a stirring solution of dioxane: H<sub>2</sub>O (4 mL) containing one of the following lanthanides at 1.1 equiv.: CeCl<sub>3</sub>, PrCl<sub>3</sub>, NdCl<sub>3</sub>, TbCl<sub>3</sub>, SmCl<sub>3</sub>, EuCl<sub>3</sub>, GdCl<sub>3</sub>, DyCl<sub>3</sub>, HoCl<sub>3</sub>, ErCl<sub>3</sub>, TmCl<sub>3</sub>, YbCl<sub>3</sub>. Metallation was monitored by UPLC/MS and upon completion was dried under reduced pressure. ESI-TOF: *m/z* C<sub>28</sub>H<sub>40</sub>N<sub>8</sub>O<sub>4</sub>Ce (M + COOH)<sup>+</sup>, calcd for 736.2455, found 736.2704. C<sub>28</sub>H<sub>40</sub>N<sub>8</sub>O<sub>4</sub>Pr (M + COOH)<sup>+</sup> calcd for 737.2147, found 737.2833. C<sub>28</sub>H<sub>40</sub>N<sub>8</sub>O<sub>4</sub>Nd (M + COOH)<sup>+</sup>, calcd for 742.2461, found 742.2865. C<sub>28</sub>H<sub>40</sub>N<sub>8</sub>O<sub>4</sub>Tb (M + COOH)<sup>+</sup>, calcd for 757.2481, found 757.3318.

C<sub>28</sub>H<sub>40</sub>N<sub>8</sub>O<sub>4</sub>Sm (M + COOH)<sup>+</sup>, calcd for 749.2346, found 749.1833. C<sub>28</sub>H<sub>40</sub>N<sub>8</sub>O<sub>4</sub>Eu (M + COOH)<sup>+</sup>, calcd for 749.2426, found 749.1849. C<sub>28</sub>H<sub>40</sub>N<sub>8</sub>O<sub>4</sub>Gd (M + COOH)<sup>+</sup>, calcd for 752.2582, found 752.3073. C<sub>28</sub>H<sub>40</sub>N<sub>8</sub>O<sub>4</sub>Dy (M + COOH)<sup>+</sup>, calcd for 756.2627, found 756.3125. C<sub>28</sub>H<sub>40</sub>N<sub>8</sub>O<sub>4</sub>Ho (M + COOH)<sup>+</sup>, calcd for 763.2531, found 763.3088. C<sub>28</sub>H<sub>40</sub>N<sub>8</sub>O<sub>4</sub>Er (M + COOH)<sup>+</sup>, calcd for 762.2672, found 762.3002. C<sub>28</sub>H<sub>40</sub>N<sub>8</sub>O<sub>4</sub>Tm (M + COOH)<sup>+</sup>, calcd for 767.2570, found 767.3286. C<sub>28</sub>H<sub>40</sub>N<sub>8</sub>O<sub>4</sub>Yb (M + COOH)<sup>+</sup>, calcd for 768.2723, found 768.3187.

#### Tetrakis(tetra-*O*-acetylglucoside) DOTAM (2)

General synthesis of Ln-2 (Ln = Gd<sup>3+</sup>, Eu<sup>3+</sup>, Dy<sup>3+</sup>, Tb<sup>3+</sup>, Tm<sup>3+</sup>). Gd-1 (40 mg, 0.057 mol) was dissolved in 2 mL 1 : 1 H<sub>2</sub>O : isopropanol and tetra-*O*-acetylglucosyl propylazide<sup>16</sup> (147 mg, 0.34 mol, 6 equiv.) was added in one portion. Copper sulfate (0.03 mol) and sodium ascorbate (0.06 mol) were added under an atmosphere of nitrogen and the mixture was stirred overnight. The product was isolated by HPLC to yield 113 mg (yield = 82%) of a colourless solid (yields: Tb<sup>3+</sup> = 68%, Tm<sup>3+</sup> = 67%, Eu<sup>3+</sup> = 75%, Dy<sup>3+</sup> = 60%). ESI-TOF: *m/z* calcd for C<sub>96</sub>H<sub>140</sub>N<sub>20</sub>O<sub>44</sub>Gd (M)<sup>3+</sup>, 802.6187, found 802.5523; calcd for C<sub>96</sub>H<sub>140</sub>N<sub>20</sub>O<sub>44</sub>Tb (M)<sup>3+</sup>, 811.9529, found 811.8862; calcd for C<sub>96</sub>H<sub>140</sub>N<sub>20</sub>O<sub>44</sub>Dy (M)<sup>3+</sup>, 812.6201, found 812.5995; calcd for C<sub>96</sub>H<sub>140</sub>N<sub>20</sub>O<sub>44</sub>Eu (M)<sup>3+</sup>, 809.2844, found 809.2227; calcd for C<sub>96</sub>H<sub>140</sub>N<sub>20</sub>O<sub>44</sub>Tm (M)<sup>3+</sup>, 815.2891, found 815.2278.

#### Deprotection of 2 to give tetraglucoside DOTAM (3)

General synthesis of Ln-3 (Ln = Gd<sup>3+</sup>, Eu<sup>3+</sup>, Dy<sup>3+</sup>, Tb<sup>3+</sup>, Tm<sup>3+</sup>). Deprotection of compound Gd-2 was done by addition of a catalytic amount of K<sub>2</sub>CO<sub>3</sub> (5 mg) to 50 mg (0.02 mmol) DOTAM glucose click in methanol. The reaction was stirred 1.5 h and then Amberlite 120 resin was then added and mixture was stirred for an additional 30 min. The solvent was filtered and dried to yield 35 mg (yield of Ln-3 = 99%) of deacetylated complex Gd-3. ESI-TOF: *m/z* calcd for C<sub>64</sub>H<sub>108</sub>N<sub>20</sub>O<sub>28</sub>Gd (M)<sup>3+</sup>, 586.8931, found 586.8877; calcd for C<sub>64</sub>H<sub>108</sub>N<sub>20</sub>O<sub>28</sub>Tb (M)<sup>3+</sup>, 587.8991, found 587.8998; calcd

for  $C_{64}H_{108}N_{20}O_{28}Dy(M)^{3+}$ , 589.5684, found 589.5697; calcd for  $C_{64}H_{108}N_{20}O_{28}Eu(M)^{3+}$ , 585.2280, found 585.2267; calcd for  $C_{64}H_{108}N_{20}O_{28}Tm(M)^{3+}$ , 591.2320, found 591.2290.

## Conclusion

We have synthesised and characterised a series of lanthanide tetraalkyne DOTAM complexes. Solution phase  $^1H$  NMR and solid state structures indicate that only SAP geometry is present in these compounds, which is useful for the development of magnetic resonance spectroscopy (MRS) and is critical for paramagnetic chemical exchange saturation transfer (ParaCEST) MR imaging agents. The complexes **Tm-1**, **Dy-1** and **Tb-1** show strong CEST signals due to the exchangeable amide protons at 25 °C, at 10 mM, pH 7. A response of 40% is observed for **Eu-1** at 51 ppm along with a significant CEST effect (~5%) due to metal-bound water which was observed for **Tb-1** and **Dy-1** at -640 and -765 ppm, respectively. Complexes producing such highly shifted signals are of interest in the development of ParaCEST contrast agents that are free of interference from background magnetization transfer effects.

We have also used “click” chemistry to functionalize the central ligand in good yields *en route* to the development of targeted contrast agents. Relaxivity measurements were used to characterize the gadolinium-containing parent and derivative agents. All of these agents possess smaller  $r_1$  values than the carboxylate ligand DOTA, which is expected on the basis of slower water exchange in the DOTAM complexes. CEST experiments were performed on **Tm-(2,3)**, **Tb-(2,3)**, **Dy-(2,3)**, and **Eu-(2,3)**. **Tm-3** shows a significant amide CEST response and **Eu-(2,3)** show promising results for bound water. However, the  $Dy^{3+}$  and  $Tb^{3+}$  complexes did not have any observable CEST response for either the amide protons or bound water.

Previous studies have shown that tumour cells have an increased demand for glucose;<sup>15,16</sup> bearing this in mind, we have pursued a flexible “click” chemistry synthetic protocol for multivalent carbohydrate decorated as potential targeted MR contrast agents.

## Acknowledgements

The authors thank the Ontario Institute for Cancer Research (OICR) for financial support of this work. We also thank Dr Francisco Martinez for collecting the NMRD data.

## Notes and references

- C. Geraldes and S. Laurent, *Contrast Media Mol. Imaging*, 2009, **4**, 1–23.
- A. X. Li, R. H. E. Hudson, J. W. Barrett, C. K. Jones, S. H. Pasternak and R. Bartha, *Magn. Reson. Med.*, 2008, **60**, 1197–1206.
- S. Aime, S. G. Crich, E. Gianolio, G. B. Giovenzana, L. Tei and E. Terreno, *Coord. Chem. Rev.*, 2006, **250**, 1562–1579.
- M. Woods, E. W. C. Donald and A. D. Sherry, *Chem. Soc. Rev.*, 2006, **35**, 500–511.
- K. M. Ward, A. H. Aletras and R. S. Balaban, *J. Magn. Reson.*, 2000, **143**, 79–87.
- S. Aime, A. Barge, J. I. Bruce, M. Botta, J. A. K. Howard, J. M. Moloney, D. Parker, A. S. de Sousa and M. Woods, *J. Am. Chem. Soc.*, 1999, **121**, 5762–5771.
- P. Caravan, J. J. Ellison, T. J. McMurphy and R. B. Lauffer, *Chem. Rev.*, 1999, **99**, 2293–2352.
- K. J. Miller, A. A. Saherwala, B. C. Webber, Y. Wu, A. D. Sherry and M. Woods, *Inorg. Chem.*, 2010, **49**, 8662–8664.
- M. M. Ali, G. S. Liu, T. Shah, C. A. Flask and M. D. Pagel, *Acc. Chem. Res.*, 2009, **42**, 915–924.
- S. Aime, A. Barge, M. Botta, A. S. De Sousa and D. Parker, *Angew. Chem., Int. Ed.*, 1998, **37**, 2673–2675.
- D. A. Fulton, E. M. Elemento, S. Aime, L. Chaabane, M. Botta and D. Parker, *Chem. Commun.*, 2006, 1064–1066.
- M. Gottschaldt and U. S. Schubert, *Chem.–Eur. J.*, 2009, **15**, 1548–1557.
- C. F. G. C. Geraldes, K. Djanashvili and J. A. Peters, *Future Med. Chem.*, 2010, **2**, 409–425.
- J. P. Andre, C. Geraldes, J. A. Martins, A. E. Merbach, M. I. M. Prata, A. C. Santos, J. J. P. de Lima and E. Toth, *Chem.–Eur. J.*, 2004, **10**, 5804–5816.
- R. A. Gatenby and R. J. Gillies, *Nat. Rev. Cancer*, 2004, **4**, 891–899.
- R. J. Gillies, N. Raghunand, G. S. Karczmar and Z. M. Bhujwala, *J. Magn. Reson. Imaging*, 2002, **16**, 430–450.
- M. Woods, A. Pasha, P. Zhao, G. Tircso, S. Chowdhury, G. Kiefer, D. E. Woessner and A. D. Sherry, *Dalton Trans.*, 2011, **40**, 6759–6764.
- J. Martinelli, B. Balali-Mood, R. Panizzo, M. F. Lythgoe, A. J. P. White, P. Ferretti, J. H. G. Steinke and R. Vilar, *Dalton Trans.*, 2010, **39**, 10056–10067.
- M. Milne, M. Suchy, A. X. Li, R. Bartha and R. H. E. Hudson, *Canadian Society for Chemistry National Conference and Exhibition*, Toronto, Ontario, Canada, 2010.
- P. Antoni, M. Malkoch, G. Vamvounis, D. Nystrom, A. Nystrom, M. Lindgren and A. Hult, *J. Mater. Chem.*, 2008, **18**, 2545–2554.
- M. P. M. Marques, C. Geraldes, A. D. Sherry, A. E. Merbach, H. Powell, D. Pubanz, S. Aime and M. Botta, *J. Alloys Compd.*, 1995, **225**, 303–307.
- H. C. Kolb, M. G. Finn and K. B. Sharpless, *Angew. Chem., Int. Ed.*, 2001, **40**, 2004–2021.
- J. A. F. Joosten, V. Loimaranta, C. C. M. Appeldoorn, S. Haataja, F. A. El Maate, R. M. J. Liskamp, J. Finne and R. J. Pieters, *J. Med. Chem.*, 2004, **47**, 6499–6508.
- S. Aime, M. Fasano and E. Terreno, *Chem. Soc. Rev.*, 1998, **27**, 19–29.
- C. A. Chang, L. C. Francesconi, M. F. Malley, K. Kumar, J. Z. Gougoutas, M. F. Tweedle, D. W. Lee and L. J. Wilson, *Inorg. Chem.*, 1993, **32**, 3501–3508.